Continuous-Discrete Cubature Kalman Filter with Log-Euclidean Metric-based Covariance Integration

Jiaolong Wang, Chengxi Zhang, Choon Ki Ahn, *Senior Member, IEEE*, Jin Wu, and Ming Liu, *Senior Member, IEEE*

***Abstract*—For continuous-discrete filtering with strong nonlinearity and large measurement intervals, a Log-Euclidean metric (LEM) based novel continuous-discrete cubature Kalman filter (LEMCDCKF) is proposed by shifting the cubature rule-based covariance propagation to Riemannian manifold. In conventional CDCKFs, the covariance differential equation based on cubature points is solved with Euclidean space integration schemes, which inevitably ignore the geometric property and restrict the performance of CDCKF. To remedy this shortage, we propose to define covariance on Riemannian symmetric positive definite (SPD) manifold and integrate the cubature rule-based covariance differential equation with the LEM-based novel scheme, which can successfully account for the manifold property of covariance matrices and provide accurate results. Moreover, by refining CDCKF with the LEM based scheme, the proposed LEMCDCKF shifts the covariance integration process to SPD manifold, which can break through the limitation of Euclidean numerical scheme. Numerical investigations verify the superior performance of the proposed LEMCDCKF in air traffic control scenarios with large measurement intervals.**

***Index Terms*—Nonlinear continuous-discrete system, cubature Kalman filter, Log-Euclidean metric, covariance propagation, symmetric positive definite.**

I. Introduction

KALMAN filter and its variants are fundamental and widely used in industrial applications [1]–[4]. But, in real application of the various Kalman type filters, the physical nature of model dynamics is usually continuous with discrete measurement outputs [5]–[8]. Hence, it is preferable to describe the continuous dynamic as a nonlinear stochastic differential equation (SDE) and the measurements as a discrete function with observation noise [9], [10], i.e. the *continuous-discrete stochastic system* with following form [7], [8], [11]:

$$\mathrm{d}x(t) = f\left(x(t)\right)\mathrm{d}t + G_t\mathrm{d}\omega(t), \tag{1}$$

$$y_k = h\left(x(t_k)\right) + v_k, \tag{2}$$

where $x(t) \in \mathbb{R}^n$ is the state to be estimated at time $t > 0$ and $y_k \in \mathbb{R}^m$ is the measurement for $x(t_k)$ at time $t_k (k = 1, 2, ...)$; $f : \mathbb{R}^n \to \mathbb{R}^n$ and $h : \mathbb{R}^n \to \mathbb{R}^m$ are respectively the nonlinear dynamic and measurement model; $G_t \in \mathbb{R}^{n\times q}$ is the known diffusion matrix; $\{\omega(t) \in \mathbb{R}^q, t > 0\}$ is the Brownian motion and the increment $\mathrm{d}\omega(t)$ is a zero-mean Gaussian white process with covariance $Q_t\mathrm{d}(t)$; $v_k \in \mathbb{R}^m$ is the zero-mean Gaussian white measurement noise with covariance R_k; the initial state $x(t_0)$ is statistically independent from above noises and also Gaussian white with mean x_{t_0} and covariance P_{t_0}.

The Kalman type estimation problem for system (1) and (2) is termed as *nonlinear continuous-discrete Kalman filtering* (NCDKF) [12], [13]. And the propagation of state and covariance between consecutive measurements requires continuously solving the coupled *moment differential equations* (MDEs) and *Fokker-Planck-Kolmogorov partial differential equation* [14], [15], rendering it difficult to handle strong model nonlinearity and rare measurements [16]–[18]. The most common idea to avoid integrating nonlinear MDE is to discretize SDE with numerical schemes and solve it with typical nonlinear Kalman filters [19], such as the discrete-discrete extended Kalman filter, discrete-discrete unscented Kalman filter, and the Itô-Taylor cubature Kalman filter [20]. However, these methods only calculate the state distribution of discrete instants and might lose the continuous nature of dynamics [12], [21].

Generally, integration and transformation schemes are employed in NCDKF to numerically solve the nonlinear MDEs [8], [17]. For example, continuous-discrete extended Kalman filter (CDEKF) linearizes the SDE to obtain a local approximation to the coupled MDEs [20]. In continuous-discrete unscented Kalman filter and cubature Kalman filter (CDCKF), the nonlinear MDEs are calculated as the weighted form of the nonlinear SDE with each sampling point, which is intended for filtering with complex nonlinearity and large intervals [9], [16]. Nevertheless, the precision of numerically solving MDEs is critical for predicting the state and covariance in NCDKF. Recursive integration and/or high-order schemes with error regulation have been employed to reduce potential errors [7], [19], and *ad hoc* techniques such as the square root version are used to improve numerical accuracy and stability [17], [19].

Note that, state covariance actually belong to the Riemannian manifold of symmetric positive definite (SPD) matrices, but above methods simply integrate the covariance differential equation in Euclidean space and ignore the geometric property of covariance propagation, restricting the estimation performance [18], [22]. In [23], the covariance differential equation of CDEKF was resolved according to the Log-Euclidean metric (LEM). However, the Taylor-series-based linearization in CDEKF might fail to work for filtering problems with strong

This work was supported in part by the Fundamental Research Funds for Central Universities (No.JUSRP121022, JUSRP123063) and the National Research Foundation of Korea (NRF) grant funded by the Korea government (Ministry of Science and ICT) (No. NRF-2020R1A2C1005449).(*Corresponding author: C. Zhang; C. K. Ahn.*)

J. Wang and C. Zhang are with the School of Internet of Things Engineering, Jiangnan University, Wuxi, China. (e-mail: jlwang@jiangnan.edu.cn; dongfangxy@163.com).

C. K. Ahn is with the School of Electrical Engineering, Korea University, Seoul 136-701, South Korea (e-mail: hironaka@korea.ac.kr).

J. Wu and M. Liu are with the Department of Electronic and Computer Engineering, Hong Kong University of Science and Technology, Hong Kong, China. (email: jin_wu_uestc@hotmail.com;eelium@ust.hk)

model nonlinearity and sparse measurements.

Given above discussion, this work proposes the LEM based novel CDCKF (LEMCDCKF) specifically for continuous-discrete systems with strong model nonlinearity and large measurement intervals. By proposing the LEM-based covariance integration scheme, LEMCDCKF shifts the cubature rule-based covariance propagation process of CDCKF onto the Riemannian manifold of SPD matrices, which can remedy the theoretical drawback of Euclidean space numerical integration in conventional CDCKF [7], [10]. The main contributions are:

1) By defining the covariance of CDCKF on SPD manifold, this work proposes to integrate the cubature rule-based covariance differential equation with the LEM-based novel scheme, which can well maintain the geometric constraint of SPD manifold and achieve better accuracy than the Euclidean space methods [10], [12], [20].
2) By embedding LEM-based integration with the Runge-Kutta scheme, the proposed LEMCDCKF can break through the bottleneck of Euclidean space numerical schemes; furthermore, the simulation results verify LEMCDCKF's superior accuracy compared with conventional CDCKF [7], [10], especially for strongly nonlinear systems with sparse measurements.

In the remainder of this work, Section II introduces the CDCKF with Euclidean space integration scheme. Section III proposes the LEM-based covaraince integration scheme for new approach LEMCDCKF. Simulation results are presented in Section IV, followed by the conclusion in Section V.

II. Conventional CDCKF with Covariance Propagation in Euclidean Space

CDCKF is originally designed for continuous-discrete systems with strong nonlinearity and large intervals [17], [19]. This section provides an introduction to the conventional CDCKF steps of numerically solving the covariance differential equation with Euclidean space Runge-Kutta scheme.

The state and covariance prediction steps of CDCKF require solving the cubature rule-based nonlinear MDEs [21]:

$$\frac{\mathrm{d}m_t}{\mathrm{d}t} = \Xi(m_t, t) \triangleq \frac{1}{2n}\sum_{i=1}^{2n} f\left(m_t + S_t\xi_i, t\right), \tag{3}$$

$$\begin{aligned}\frac{\mathrm{d}P_t}{\mathrm{d}t} &= \Psi(P_t, m_t, t)\\ &\triangleq \frac{1}{2n}\sum_{i=1}^{2n}\left[\begin{array}{c} f\left(m_t + S_t\xi_i, t\right)S_t\xi_i^\top \\ +S_t\xi_i f^\top\left(m_t + S_t\xi_i, t\right)\end{array}\right] + G_tQ_tG_t^\top,\end{aligned} \tag{4}$$

where $\xi_i = \sqrt{n}\left\{\begin{array}{cc} e_i & i = 1, 2, ..., n \\ -e_{i-1} & i = n+1, ..., 2n\end{array}\right.$ are the cubature rule sampling points with e_i indicating the ith coordinate base vector of $\mathbb{R}^n$; S_t denotes the lower-triangular matrix satisfying $P_t = S_tS_t^\top$ with $\top$ denoting the transpose operator. To integrate the cubature rule-based MDE (3) and (4) from t_{k-1} to t_k, the initial conditions are $m_{t_{k-1}} = \hat{x}_{k-1|k-1}$ and $P_{t_{k-1}} = P_{k-1|k-1}$, where $\hat{x}_{k-1|k-1}$ and $P_{k-1|k-1}$ are respectively the posterior estimate and covariance at time instant t_{k-1} [14]. The prior estimate $\hat{x}_{k|k-1}$ and covariance $P_{k|k-1}$ can be determined with $\hat{x}_{k|k-1} = m_{t_k}$ and $P_{k|k-1} = P_{t_k}$. Then, given the discrete measurements, the correction stage can be conducted as typical cubature Kalman filter. Note that, square root algorithms integrate the lower-triangular S_t to ensure numerical symmetry [12], [17].

Obviously, CDCKF's performance heavily depends on the numerical accuracy and stability of integrating the cubature rule-based MDEs (3) and (4), especially for strong model nonlinearity and large measurement intervals. Dividing interval $\Delta t = t_k - t_{k-1}$ into N intermediates as $t_{k-1} = t_{k-1,1} < \cdots < t_{k-1,i} < \cdots < t_{k-1,N} = t_k$ and using higher-order integration schemes are beneficial ways of improving the numerical precision [17], [19]. For example, using fourth-order Runge-Kutta scheme, (3) and (4) can be numerically integrated for sub-interval $\delta_i = t_{k-1,i+1} - t_{k-1,i}$ as

$$\begin{aligned}
&K_1^m = \Xi(m_{t_{k-1,i}}, t_{k-1,i}),\\
&K_1^P = \Psi(P_{t_{k-1,i}}, m_{t_{k-1,i}}, t_{k-1,i}),\\
&K_2^m = \Xi(m_{t_{k-1,i}} + \delta_iK_1^m/2, t_{k-1,i} + \delta_i/2),\\
&K_2^P = \Psi(P_{t_{k-1,i}} + \delta_iK_1^P/2, m_{t_{k-1,i}} + \delta_iK_1^m/2, t_{k-1,i} + \delta_i/2),\\
&K_3^m = \Xi(m_{t_{k-1,i}} + \delta_iK_2^m/2, t_{k-1,i} + \delta_i/2),\\
&K_3^P = \Psi(P_{t_{k-1,i}} + \delta_iK_2^P/2, m_{t_{k-1,i}} + \delta_iK_2^m/2, t_{k-1,i} + \delta_i/2),\\
&K_4^m = \Xi(m_{t_{k-1,i}} + \delta_iK_3^m, t_{k-1,i} + \delta_i),\\
&K_4^P = \Psi(P_{t_{k-1,i}} + \delta_iK_3^P, m_{t_{k-1,i}} + \delta_iK_3^m, t_{k-1,i} + \delta_i),\\
&m_{t_{k-1,i+1}} = m_{t_{k-1,i}} + \delta_i\left(K_1^m + 2K_2^m + 2K_3^m + K_4^m\right)/6,\\
&P_{t_{k-1,i+1}} = P_{t_{k-1,i}} + \delta_i\left(K_1^P + 2K_2^P + 2K_3^P + K_4^P\right)/6,
\end{aligned}$$

where K_j^m, $K_j^P (j = 1, 2, 3, 4)$ are intermediate terms. Besides, high-order implicit integration schemes with error regulator have been used to improve CDCKF's precision [7], [10].

Problem: In above numerical implementation of CDCKF, the cubature rule-based covariance differential equation (4) is simply treated as an Euclidean matrix differential equation. However, the SPD covariance matrices only constitute the interior of a convex cone in the Euclidean vector matrix space, i.e. the Riemannian manifold of SPD matrices [24]. Therefore, solving the cubature rule-based covariance differential equation (4) with Euclidean space integration schemes will violate the geometric structure of SPD manifold and produce inaccurate results [23]. For example, the Euclidean addition of the covariance matrix with negative symmetry matrices may be non-SPD, which is often encountered by conventional CDCKF [12]. Although higher-order numerical schemes and/or extra *ad hoc* techniques can improve the numerical accuracy to some extent, they are still Euclidean space methods and cannot well keep the geometry nature of manifold, which will inevitably confine the performance of CDCKF.

III. Continuous-Discrete CKF with LEM-based Covariance Integration on SPD Manifold

To accurately preserve the manifold nature of covariance, we propose the LEM based novel scheme to accurately integrate the cubature rule-based covariance differential equation (4), which constitutes the key innovation of LEMCDCKF.

A. Covariance Propagation on Riemannian SPD Manifold

The covariance P_t in Kalman theory naturally belongs to the Riemannian manifold $Sym^+(n)$ of $n \times n$ SPD matrices, while

the tangent $\mathrm{d}P_t/\mathrm{d}t = \Psi(P_t, m_t, t)$ evolves on the manifold of $n \times n$ symmetric matrices $Sym(n)$ [18], [24]. According to manifold theory, there is a local diffeomorphism between $Sym^+(n)$ and the tangent space $T_{P_t}Sym^+(n)$ based on the matrix exponential expm and logarithm logm:

$$Sym(n) = T_{P_t}Sym^+(n) \underset{\text{logm}}{\overset{\text{expm}}{\rightleftharpoons}} Sym^+(n).$$

Therefore, the "addition" and "subtraction" on $Sym^+(n)$ can be conducted using its diffeomorphism with $Sym(n)$ and the manipulation of $P_t, P_{t+\delta} \in Sym^+(n)$ can be interpreted as

$$\overrightarrow{P_tP_{t+\delta}} \triangleq \text{logm}(P_{t+\delta}) - \text{logm}(P_t) \in Sym(n), \quad (5)$$

$$P_{t+\delta} = \text{expm}\left(\text{logm}(P_t) + \overrightarrow{P_tP_{t+\delta}}\right) \in Sym^+(n), \quad (6)$$

which can help generalize the conventional numerical integration schemes of Euclidean space to the Riemannian manifold [18]. Note that, tangent space $T_{P_t}Sym^+$ is aligned at manifold point P_t; hence, a diffeomorphism is one-to-one only locally around P_t with a small increment δ. Then, as $\delta \to 0$,

$$\frac{\overrightarrow{P_tP_{t+\delta}}}{\delta} = \frac{\text{logm}\left(P_{t+\delta}\right) - \text{logm}\left(P_t\right)}{\delta} \simeq \frac{\text{dlogm}\left(P_t\right)}{\mathrm{d}t_t}, \quad (7)$$

where the Riemannian metric of LEM is used to evaluate the "distance" on the manifold [24]. Here, δ is determined by the measurement interval Δt and the number N of intermediate instants. Therefore, to approximate the derivative for LEM, a scalar α with $0 < \alpha \ll 1$ and the incremental estimate $P_t + \alpha\delta\mathrm{d}P_t/\mathrm{d}t$ can be employed as

$$\frac{\text{dlogm}(P_t)}{\mathrm{d}t} \simeq \frac{\text{logm}\left(P_t + \alpha\delta\mathrm{d}P_t/\mathrm{d}t\right) - \text{logm}\left(P_t\right)}{\alpha\delta}. \quad (8)$$

Then with (6) and (7), as $\alpha, \delta \to 0$, we have

$$\overrightarrow{P_tP_{t+\delta}} \simeq \frac{\text{logm}\left(P_t + \alpha\delta\mathrm{d}P_t/\mathrm{d}t\right) - \text{logm}\left(P_t\right)}{\alpha}, \quad (9)$$

$$P_{t+\delta} = \text{expm}\left(\text{logm}(P_t) + \overrightarrow{P_tP_{t+\delta}}\right) \simeq$$

$$\text{expm}\left(\frac{\text{logm}\left(P_t + \alpha\delta\mathrm{d}P_t/\mathrm{d}t\right) - (1-\alpha)\text{logm}(P_t)}{\alpha}\right). \quad (10)$$

B. CDCKF with Accurate Covariance Integration on Manifold

With the proposed (10) as the basic first order implementation, higher order Euclidean numerical schemes can be generalized onto SPD manifold. For example, with the intermediate steps $t_{k-1} = t_{k-1,1} < \cdots < t_{k-1,i} < \cdots < t_{k-1,N} = t_k$, the fourth-order Runge-Kutta scheme of Section II-B can be extended for covariance manipulation on the manifold. From $t_{k-1,i}$ to $t_{k-1,i+1}$, the K_j^m $(j = 1, 2, 3, 4)$, K_1^P and $m_{t_{k-1,i+1}}$ are same as Section II, but the calculus for terms K_2^P, K_3^P, K_4^P should be substituted with

$$\begin{aligned}
L_1 &= \text{logm}\left(P_{t_{k-1,i}} + \alpha\delta_i K_1^P/2\right) - (1-\alpha)\text{logm}\left(P_{t_{k-1,i}}\right),\\
K_2^P &= \Psi\left(\text{expm}(L^1/\alpha), m_{t_{k-1,i}} + \delta_i K_1^m/2, t_{k-1,i} + \delta_i/2\right),\\
L_2 &= \text{logm}\left(P_{t_{k-1,i}} + \alpha\delta_i K_2^P/2\right) - (1-\alpha)\text{logm}\left(P_{t_{k-1,i}}\right),\\
K_3^P &= \Psi\left(\text{expm}(L^2/\alpha), m_{t_{k-1,i}} + \delta_i K_2^m/2, t_{k-1,i} + \delta_i/2\right),\\
L_3 &= \text{logm}\left(P_{t_{k-1,i}} + \alpha\delta_i K_3^P\right) - (1-\alpha)\text{logm}\left(P_{t_{k-1,i}}\right),\\
K_4^P &= \Psi\left(\text{expm}(L^3/\alpha), m_{t_{k-1,i}} + \delta_i K_3^m, t_{k-1,i} + \delta_i\right),
\end{aligned}$$

so the final calculus of $P_{t_{k-1,i+1}}$ in Section II is refined as

$$\begin{aligned}
M_1 &= \left[\text{logm}\left(P_{t_{k-1,i}} + \alpha\delta_i K_1^P/6\right) - (1-\alpha)\text{logm}\left(P_{t_{k-1,i}}\right)\right]/\alpha,\\
M_2 &= \left[\text{logm}\left(\text{expm}\left(M_1\right) + \alpha\delta_i K_2^P/3\right) - (1-\alpha)\,M_1\right]/\alpha,\\
M_3 &= \left[\text{logm}\left(\text{expm}\left(M_2\right) + \alpha\delta_i K_3^P/3\right) - (1-\alpha)\,M_2\right]/\alpha,\\
M_4 &= \left[\text{logm}\left(\text{expm}\left(M_3\right) + \alpha\delta_i K_4^P/6\right) - (1-\alpha)\,M_3\right]/\alpha,\\
P_{t_{k-1,i+1}} &= \text{expm}\left(M_4\right),
\end{aligned}$$

which provides the LEM-based Runge-Kutta scheme specifically for accurate covariance integration on SPD manifold. Note that, in the final calculus of Section II $P_{t_{k-1,i}}$ is added with the weighted Euclidean space summation of $K_j^P, (j = 1, 2, 3, 4)$. But in above proposed calculus, K_j^P is recursively injected to propagate the intermediate M_1, M_2, M_3 and the final one for $P_{t_{k-1,i+1}}$ with M_4 is actually obtained based on M_1, M_2, M_3. In this sense, the main difference of proposed implementation of fourth-order Runge-Kutta is that the original $P_{t+\delta} = P_t + \delta\Psi(P_t, m_t, t)$ is replaced by scheme (10).

C. Summary Discussions about Proposed LEMCDCKF

In the proposed LEMCDEKF, the key innovation to CDCKF are the LEM-based new scheme (10) and the resulting novel manifold Rung-Kutta scheme for accurately solving the cubature rule-based covariance differential equation (4). It should be noted that although the covariance obtained by the matrix exponential is naturally SPD, in the logarithm operations for calculating L_j $(j = 1, 2, 3)$, the terms with P_t and $\alpha\delta_i K_j^P$ should be strictly SPD or the logarithm would break down. For example, a proper α should guarantee the positiveness of $(P_t + \alpha\delta\mathrm{d}P_t/\mathrm{d}t)$ for the $\text{logm}(P_t + \alpha\delta\mathrm{d}P_t/\mathrm{d}t)$ of (10). Given the initial $P_t > 0$, if $\mathrm{d}P_t/\mathrm{d}t$ is positive or semi-positive definite, we always have $P_t + \alpha\delta\mathrm{d}P_t/\mathrm{d}t > 0$. But, if the least eigenvalue of $\mathrm{d}P_t/\mathrm{d}t$ is negative, i.e. $\lambda_{\min}\left(\mathrm{d}P_t/\mathrm{d}t\right) < 0$, then the conservative condition $\lambda_{\min}\left(P_t\right) > -\alpha\delta\lambda_{\min}\left(\mathrm{d}P_t/\mathrm{d}t\right)$ can be used to tune the parameter $\alpha > 0$ and $\delta > 0$.

As to the computational cost, the numerical implementation of the proposed manifold Runge-Kutta scheme extra requires 7 matrix exponential and 6 matrix logarithm operations (the logarithm $\text{logm}\left(P_{t_{k-1,i}}\right)$ for calculating L_1 can be initialized with the M_4 of previous integration step), and so it is necessary to simplify their numerical complexity. Note that, the covariance matrix $P \in Sym^+(n)$ with full eigenvector matrix V and diagonal eigenvalues $\lambda_1, \lambda_2, .., \lambda_n$ can be factorized as $P = V\text{diag}(\lambda_1, \lambda_2, .., \lambda_n)V^{-1}$; hence, the matrix exponential and logarithm operations can be mathematically converted into multiple scalar operation log and exp as follows,

$$\begin{aligned}
D &\triangleq \text{logm}(P) = \text{logm}\left(V\text{diag}(\lambda_1, \lambda_2, .., \lambda_n)V^{-1}\right)\\
&= V\text{logm}(\text{diag}(\lambda_1, \lambda_2, .., \lambda_n))V^{-1}\\
&= V\text{diag}(\log\lambda_1, \log\lambda_2, .., \log\lambda_n)V^{-1}\\
&= V\text{diag}(d_1, d_2, .., d_n)V^{-1},\\
P &= \text{expm}(D) = V\text{expm}(\text{diag}(d_1, d_2, .., d_n)V^{-1}\\
&= V\text{diag}(\text{exp}d_1, \text{exp}d_2, .., \text{exp}d_n))V^{-1}.
\end{aligned}$$

This article has been accepted for publication in IEEE Transactions on Circuits and Systems--II: Express Briefs. This is the author's version which has not been fully edited and content may change prior to final publication. Citation information: DOI 10.1109/TCSII.2023.3279140

Further, proper approximations can help improve the algorithm efficiency of exponential and logarithm. For example,

$$\exp(d_i) = \lim_{b\to\infty}\left(1+\frac{d_i}{b}\right)^b,$$

In summary, the cubature rule-based MDE (4) of CDCKF is not a regular matrix differential equation in Euclidean space and conventional numerical schemes might violate the manifold nature and restrict the accuracy of covariance integration. By shifting the covariance integration from Euclidean space to the Riemannian manifold, the proposed LEMCDCKF can well preserves the manifold geometry and break through the performance bottleneck of conventional CDCKF.

IV. Numerical Analysis

This section investigates the performance of LEMCDEKF using numerical simulations of the air traffic control scenario, which is the benchmark application of radar tracking systems to estimate the position and velocity of an maneuvering aircraft [7], [10], [16], [19]. The radar tracking systems for aircraft's coordinated turn dynamics with Brownian motion noise can be modeled as a typical continuous-discrete filtering problem. For the SDE (1),$f(x_t) = [\dot{\alpha}, -\omega\dot{\beta}, \dot{\beta}, \omega\dot{\alpha}, \dot{\gamma}, 0, 0]^\top \in \mathbb{R}^7$ and $x_t = [\alpha, \dot{\alpha}, \beta, \dot{\beta}, \gamma, \dot{\gamma}, \omega]^\top \in \mathbb{R}^7$ with α, β, γ and $\dot{\alpha}, \dot{\beta}, \dot{\gamma}, \omega$ representing the 3D position (m), velocity (m/s) and turn rate($^\circ/s$). Moreover, $w_t \in \mathbb{R}^7$ is with diffusion matrix $G_t = I_7$ and $Q_t = \mathrm{diag}([0, 0.2, 0, 0.2, 0, 0.2, 0.000049])$. $h(x_k) = \left[\sqrt{\alpha_k^2+\beta_k^2+\gamma_k^2}, \tan^{-1}(\beta_k/\alpha_k), \tan^{-1}\left(\gamma_k/\sqrt{\alpha_k^2+\beta_k^2}\right)\right]^\top$ with $R_k = \mathrm{diag}([2500, 0.01, 0.01])$ and measurement interval Δt. The true continuous states for SDE (1) are generated by the Euler-Maruyama method using a time increment of 1 μs for 210s with the initial condition of state $x_{t_0} = [1000, 0, 2650, 150, 200, 0, 6]^T$ and covariance $P_{t_0} = [20, 0.02, 10, 0.01, 5, 0.005, 0.01]^T$.

The LEMCDCKF with $\alpha = 0.01$ was compared with the Runge-Kutta-based DD extended Kalman filter (DDEKF) and CDEKF [20],nthe Runge-Kutta-based CDCKF [9], the Runge-Kutta-based NCDCKF [16], the Itô-Taylor 1.5 based ItoCDCKF [19], and the LEMCDEKF that embeds the LEM-based scheme into CDEKF. The random state was initialized with Gaussian mean x_{t_0} and covariance P_{t_0}. Since the research topic of this work is to improve the state estimation precision of nonlinear continuous-discrete filtering problem, so it is necessary to evaluate the final ARMSE results of proposed LEMCDCKF and other methods. A total of 100 Monte Carlo simulations with true trajectories and measurements and the average root-mean-square error (ARMSE) of the 3D position [15] were calculated as the evaluation metric:

1) With constant δ_i= 0.002s ($N = 500\Delta t$) for the numerical Runge-Kutta scheme, the ARMSE results of all filters for the large interval $\Delta t = 5 \sim 30$ are given in Fig. 1.
2) With measurement interval Δt= 10 or 30s, the ARMSE results for the intermediate number $N = 300 \sim 1000\Delta t$ are respectively displayed in Figs. 2 and 3.

According to above ARMASE results, we can arrive at the following conclusions about the filtering performance.

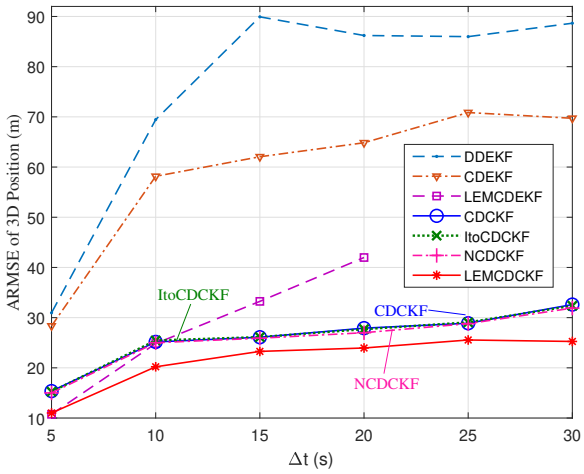

Fig. 1. ARMSE results of 3D position for different filtering methods with large intervals of $\Delta t = 5s, 10s, 15s, 20s, 25s, 30s$.

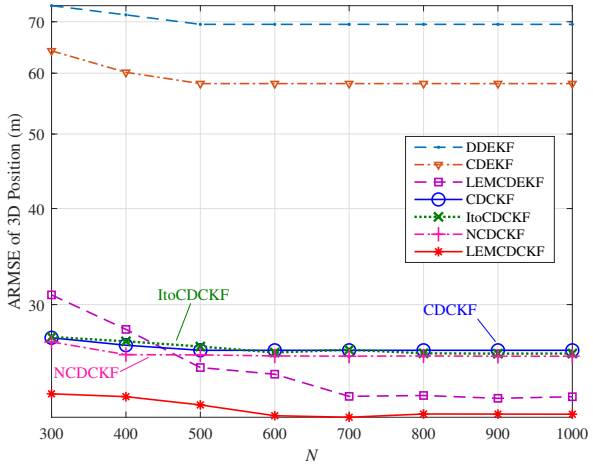

Fig. 2. ARMSE results of 3D position for different filtering methods with $\Delta t = 10s$ and $N = 300 \sim 1000\Delta t$.

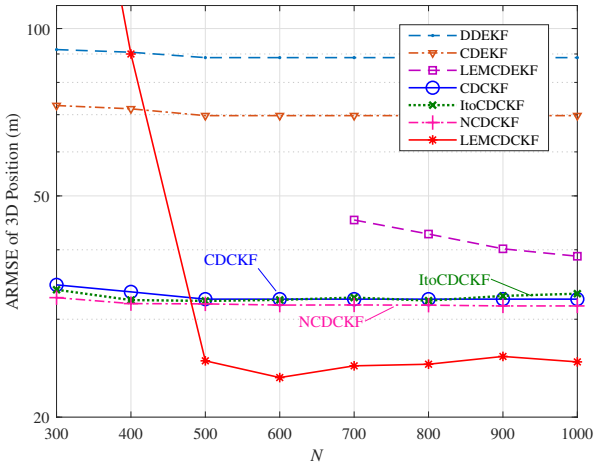

Fig. 3. ARMSE results of 3D position for different filtering methods with $\Delta t = 30s$ and $N = 300 \sim 1000\Delta t$.

1) With the same condition δ_i=0.002s (i.e. $N = 500\Delta t$), the proposed LEMCDCKF exhibited better estimation accuracy than the other methods for filtering with large measurement intervals $\Delta t = 5 \sim 30$, as shown in Fig. 1. For interval $\Delta t = 5$, although LEMCDEKF can provide similar results to LEMCDCKF, it degrades quickly for larger Δt and even diverges for $\Delta t > 20$. The ARMSE results of CDCKF, NCDCKF and ItoCDCKF were obviously larger than that of LEMCDCKF.
2) The ARMSE results of CDEKF, DDEKF, CDCKF, NCDCKF and ItoDDCKF were nearly constant for $N \geq 500$ (Figs. 2 and 3). This demonstrated that they had achieved their performance limit of estimation accuracy and even a larger N could not produce any improvement. Accordingly, with the LEM-based propagation scheme, the proposed LEMCDCKF can effectively break through the theoretical restriction of Euclidean space integration schemes, confirming the discussions in Section III-C.
3) For the cases of larger integration interval $\Delta t = 30$ in Fig. 3, with $N < 500\Delta t$ the sub-interval δ_i was not sufficiently small to ensure the required accuracy condition for the equation (7) $\sim$ (10); actually, the new scheme (10) for LEMCDCKF works well for $N \geq 500\Delta t$ while the LEMCDEKF only displays degraded accuracy for $N \geq 700\Delta t$. So, for large Δt, a smaller δ_i (larger N) is preferred for LEMCDCKF such as $N \geq 500\Delta t$.
4) For implementations using MATLAB code on a 64-bit computer with a 3.60 GHz i7-7700 CPU, the average computational cost of LEMCDCKF was approximately 2.6 times that of the conventional CDCKF due to extra usage of the matrix logarithm and exponential operations, as discussed in Section III-C.

Obviously, using the LEM-based propagation scheme, the proposed LEMCDCKF can effectively break through the restriction of the Euclidean space integration scheme in conventional methods, confirming the related discussions in Section III-C. Note that, the detailed filtering steps of general CDCKF and the proposed LEMCDCKF are all same except that their covariance propagation schemes for (4) are the critical difference between CDCKF and LEMCDCKF. Therefore, we think the improved performance of LEMCDCKF is just due to the contribution of proposed covariance propagation scheme (10) on manifold.

V. Conclusions

In this work, the LEM-based new CDCKF was proposed for continuous-discrete systems with strong nonlinearity and large measurement intervals. As the main innovation, the cubature rule-based covariance differential equation is considered on the Riemannian manifold and then propagated with the LEM-based Runge-Kutta scheme, avoiding the restrictions of the Euclidean space numerical integration scheme. Numerical simulations further demonstrated that the proposed LEMCDCKF can overcome the theoretical drawback of conventional CDCKF in Euclidean space and effectively improve estimation accuracy.

References

[1] H. Fu and Y. Cheng, "A novel robust Kalman filter based on switching gaussian-heavy-tailed distribution," *IEEE Transactions on Circuits and Systems II: Express Briefs*, vol. 69, pp. 3012–3016, 2022.

[2] X. Fan, G. Wang, J. Han, and Y. Wang, "Interacting multiple model based on maximum correntropy Kalman filter," *IEEE Transactions on Circuits and Systems II: Express Briefs*, vol. 68, pp. 3017–3021, 2021.

[3] S. H. You, C. K. Ahn, Y. S. Shmaliy, and S. Zhao, "Fusion Kalman and weighted UFIR state estimator with improved accuracy," *IEEE Transactions on Industrial Electronics*, vol. 67, pp. 10 713–10 722, 2020.

[4] Y. S. Shmaliy, F. Lehmann, S. Zhao, and C. K. Ahn, "Comparing robustness of the Kalman, H_∞ , and UFIR filters," *IEEE Transactions on Signal Processing*, vol. 66, pp. 3447–3458, 2018.

[5] S. Li, Y. Hu, L. Zheng, Z. Li, X. Chen, T. L. Fernando, H. H.-C. Iu, Q. Wang, and X. Liu, "Stochastic event-triggered cubature Kalman filter for power system dynamic state estimation," *IEEE Transactions on Circuits and Systems II: Express Briefs*, vol. 66, pp. 1552–1556, 2019.

[6] J. Xing, T. Jiang, and Y. jie Li, "q-rényi kernel functioned Kalman filter for land vehicle navigation," *IEEE Transactions on Circuits and Systems II: Express Briefs*, vol. 69, pp. 4598–4602, 2022.

[7] G. Y. Kulikov and M. V. Kulikova, "Hyperbolic-SVD-based square-root unscented kalman filters in continuous-discrete target tracking scenarios," *IEEE Transactions on Automatic Control*, vol. 67, no. 1, pp. 366–373, 2022.

[8] T. Mazzoni, "Computational aspects of continuous–discrete extended Kalman-filtering," *Computational Statistics*, vol. 23, pp. 519–539, 2008.

[9] S. Särkkä, "On unscented Kalman filtering for state estimation of continuous-time nonlinear systems," *IEEE Transactions on Automatic Control*, vol. 52, pp. 1631–1641, 2007.

[10] M. V. Kulikova and G. Y. Kulikov, "SVD-based factored-form cubature Kalman filtering for continuous-time stochastic systems with discrete measurements," *Automatica*, vol. 120, p. 109110, 2020.

[11] ——, "Continuous-discrete unscented Kalman filtering framework by matlab ode solvers and square-root methods," *Autom.*, vol. 142, p. 110396, 2022.

[12] S. Särkkä and A. Solin, "On continuous-discrete cubature Kalman filtering," *IFAC Proceedings Volumes*, vol. 45, pp. 1221–1226, 2012.

[13] Á. F. García-Fernández and W. Yi, "Continuous-discrete multiple target tracking with out-of-sequence measurements," *IEEE Transactions on Signal Processing*, vol. 69, pp. 4699–4709, 2021.

[14] G. Y. Kulikov and M. V. Kulikova, "Accurate numerical implementation of the continuous-discrete extended Kalman filter," *IEEE Transactions on Automatic Control*, vol. 59, pp. 273–279, 2014.

[15] ——, "The accurate continuous-discrete extended Kalman filter for radar tracking," *IEEE Transactions on Signal Processing*, vol. 64, pp. 948–958, 2016.

[16] J. Wang, D. Zhang, and X. Shao, "New version of continuous-discrete cubature Kalman filtering for nonlinear continuous-discrete systems." *ISA transactions*, 2019.

[17] M. V. Kulikova and G. Y. Kulikov, "Square-root filtering via covariance svd factors in the accurate continuous-discrete extended-cubature Kalman filter," *Applied Numerical Mathematics*, vol. 171, pp. 32–44, 2022.

[18] H. M. Menegaz, J. Y. Ishihara, and H. T. M. Kussaba, "Unscented Kalman filters for riemannian state-space systems," *IEEE Transactions on Automatic Control*, vol. 64, pp. 1487–1502, 2019.

[19] I. Arasaratnam, S. Haykin, and T. R. Hurd, "Cubature Kalman filtering for continuous-discrete systems: Theory and simulations," *IEEE Transactions on Signal Processing*, vol. 58, pp. 4977–4993, 2010.

[20] P. Frogerais, J.-J. Bellanger, and L. Senhadji, "Various ways to compute the continuous-discrete extended Kalman filter," *IEEE Transactions on Automatic Control*, vol. 57, pp. 1000–1004, 2012.

[21] S. Särkkä and J. Sarmavuori, "Gaussian filtering and smoothing for continuous-discrete dynamic systems," *Signal Process.*, vol. 93, pp. 500–510, 2013.

[22] S. Zhao, Y. S. Shmaliy, P. Shi, and C. K. Ahn, "Fusion Kalman/UFIR filter for state estimation with uncertain parameters and noise statistics," *IEEE Transactions on Industrial Electronics*, vol. 64, pp. 3075–3083, 2017.

[23] G. Bourmaud, R. Mégret, M. Arnaudon, and A. Giremus, "Continuous-discrete extended Kalman filter on matrix lie groups using concentrated gaussian distributions," *Journal of Mathematical Imaging and Vision*, vol. 51, pp. 209–228, 2014.

[24] K. Chen, J. Ren, X. Wu, and J. Kittler, "Covariance descriptors on a gaussian manifold and their application to image set classification," *Pattern Recognition*, vol. 107, p. 107463, 2020.